crystals

MDPI

Article

Enhanced Dissolution Efficiency of Tamoxifen Combined with Methacrylate Copolymers in Amorphous Solid Dispersions

Dayanne T. C. da Silva [1,*], Daniela Nadvorny [1], Lucas J. de A. Danda [1], Amanda C. Q. de M. Vieira [1], Patricia Severino [2,3,4], Monica F. La R. Soares [1], José L. Soares-Sobrinho [1,*] and Eliana B. Souto [5,6,*]

1 Department of Pharmaceutical Sciences, Federal University of Pernambuco, Av. Prof. Artur de Sá, s/n, CEP 50740-520 Recife, Brazil; nady@ufpe.br (D.N.); lucas.danda@ufpe.br (L.J.d.A.D.); quintas.amanda@gmail.com (A.C.Q.d.M.V.); monica.soares@ufpe.br (M.F.L.R.S.)
2 Labora and ry of Nanotechnology and Nanomedicine (LNMED), Institute of Technology and Research (ITP), Tiradentes University, 49010-390 Aracaju, Brazil; patricia_severino@itp.org.br
3 Instituto de Tecnologia e Pesquisa (ITP), Av. Murilo Dantas, 300, CEP 49032-490 Aracaju, Brazil
4 Tiradentes Institute, 150 Mt Vernon St, Dorchester, MA 02125, USA
5 Department of Pharmaceutical Technology, Faculty of Pharmacy, University of Coimbra, Polo das Ciências da Saúde Azinhaga de Santa Comba, 3000-548 Coimbra, Portugal
6 CEB—Centre of Biological Engineering, Campus de Gualtar, University of Minho, 4710-057 Braga, Portugal
* Correspondence: dayannecasimiro@hotmail.com (D.T.C.d.S.); jose.ssobrinho@ufpe.br (J.L.S.-S.); ebsouto@ff.uc.pt (E.B.S.)

Received: 10 October 2020; Accepted: 13 November 2020; Published: 17 November 2020

Abstract: Amorphous solid dispersions (SDs) containing poorly soluble tamoxifen dispersed in a meth(acrylate) copolymer combination were proposed as a controlled release system. The objective of this work was to investigate the characteristics and performance of the tamoxifen–polymer mixture and evaluate the changes in functionality through a supersaturating dissolution study condition while comparing it to a physical mixture at a fixed drug-loading proportion. Two polymers, Eudragit® L 100 and Eudragit® RL 100, were used to prepare SDs with a 1:1 polymer ratio, containing 10%, 20%, or 30% (wt/wt%) of tamoxifen, by the solvent evaporation method. A physical mixture containing 30% of tamoxifen was also prepared for comparison. SDs were characterized by X-ray diffraction, Fourier-transform infrared spectroscopy, differential scanning calorimetry, and scanning electron microscopy. Dissolution tests were conducted under non-sink conditions to verify the occurrence of drug recrystallization upon its release. Solid-state characterizations confirmed that the drug was in the amorphous state within the polymeric matrix. Tamoxifen release in an acidic medium was mainly affected by the increase in drug concentration caused by the possible loss of interactions that characterize the main polymer functionalities. At pH 7.4, supersaturation was slowly achieved while also contributing to the increase in the kinetic solubility of the drug. The physical mixture demonstrated the best overall performance, suggesting that the polymeric interactions may have negatively affected the drug release. The combination of polymers in the composing SD proved to be a promising strategy to tailor the delivery of poorly soluble drugs. Our study highlights important information on the behavior of tamoxifen as a poorly soluble drug in supersaturating dissolution conditions while released from SD systems.

Keywords: tamoxifen; solid dispersions; supersaturation; polymer blending; recrystallization

1. Introduction

Tamoxifen (TMX) is a selective modulator of estrogen receptors used as a prophylactic agent for cancer prevention. TMX is classified as a Class II drug of the Biopharmaceutical Classification System (BCS), which translates high permeability but poor aqueous solubility. The risk of TMX precipitation as a free base in the acidic environment of the stomach can cause serious complications in patients predisposed to bacterial colonization as a physical aggressor [1]. Besides, its poor aqueous solubility also interferes with the extent of absorption, since dissolution is the limiting step for drug absorption in the case of Class II drugs.

Poorly water-soluble drugs have become increasingly frequent in pharmaceutical technology pipelines. To overcome this issue, drug delivery systems (DDS) based on several different carriers have been proposed to either increase the dissolution rate or the apparent solubility of poorly soluble drugs. Among these strategies, amorphous solid dispersions (ASD) emerge as a promising DDS formed either by dissolving or dispersing the drug in an inert polymer [2–4], with increasing advantages through the proper selection of the polymeric carriers [5,6].

The choice of an ideal polymeric carrier that can overcome the limitations of ASD strategy (such as recrystallization of the amorphous drug back to its crystalline less-soluble form [7]), and attending the specific needs of a poorly water-soluble drug can be rather challenging [8]. Several methods have been proposed, e.g., by developing formulations with drug derivatives [9–11] and, also, by polymeric grafting [12], crosslinking [13–15], and through polymeric mixtures [8,16,17]. Among these strategies, polymer blending provides an alternative to the modification or synthesis of new polymers, with a diverse range of possibilities that can provide improved drug delivery properties. As such, ASDs based on polymeric mixtures, as a strategy to enhance the dissolution performance of poorly soluble drugs, has received much less attention.

Research has been focused on the analysis of combining polymers for the controlled release of drugs using acrylic polymers, such as the various forms of poly(ethylacryl ate-co-methylmethacrylate) and poly(methacrylic acid-co-ethylacrylate) [18], which are common-use FDA-approved polymers with permissible daily intakes of 2–20 mg/kg of body weight [19–23], all of which have been previously used as platforms for controlled drug releases and/or specific pH-dependent releases to achieve distinct drug profiles [20,24]. Formulations containing poly(meth)acrylate polymers that promote either a controlled release, increase in drug dissolution rate, pH-dependent release, or skin permeation have been described in several studies [25–28].

The aim of this study was to evaluate the efficacy of a TMX in vitro release from new SDs prepared with a combination of Eudragit® L 100 (a methacrylic acid copolymer insoluble at a pH below 5.5) and Eudragit® RL 100 (an insoluble methacrylic ester copolymer that swells in water) at varied drug loadings while comparing them to a physical mixture of both polymers and the poorly soluble drug. An in-vitro drug release study was conducted under non-sink conditions in order to evaluate drug release at a supersaturating environment.

2. Material and Methods

2.1. Materials

Eudragit® L 100 (batch B140703008) and Eudragit® RL 100 (batch E111006200) were donated by Evonik Degussa Brazil Ltd. (Castro, PN, Brazil). Tamoxifen citrate (99%, batch 458145), high performance liquid chromatography (HPLC) grade methanol, hydrochloric acid, and polysorbate 80 were obtained from Research Products International (Mt Prospect, IL, USA). All other chemicals and reagents were of analytical grade and were used as received.

2.2. Preparation of Solid Dispersions by Solvent Cast

Initially, a 1:1 (wt/wt%) blend solution of Eudragit® RL 100 and Eudragit® L 100 was prepared by dissolving 1 g of each polymer in methanol and continuously stirring during 30 min using a

magnetic stirrer until solution was formed (note: Eudragit® L 100 forms a slightly whitish solution). Subsequently, an accurately weighted mass of 200, 400, or 600 mg tamoxifen (TMX) was added and completely dissolved to form a 10%, 20%, or 30% (wt/wt%) drug loading solid dispersion (SD), respectively (namely, "SD 10%", "SD 20%", and "SD 30%", respectively). All systems were sonicated in an ultrasonic bath until a solution was formed. Solutions were spread onto silicone forms and dried in a conventional oven at 60 ± 2°C under atmospheric pressure for a maximum of 2 h for solvent evaporation. Then, for complete solvent evaporation, samples were dried in a vacuum oven at 60 ± 2°C. The resulting films were ground with the aid of a small quantity of liquid nitrogen to avoid drug crystallization induced by heat from friction. For comparison, a physical mixture (PM) containing 30% (wt/wt%) of TMX with both polymers at 1:1 proportions (namely, "PM 30%") was also prepared, along with a blank SD without TMX (namely, "Binary SD") with both polymers at 1:1 proportions (wt/wt). All solid powders, including crystalline TMX, were sieved through a 150-μm sieve to standardize particle size fractions. Powders were packaged in bottles and stored in a desiccator.

2.3. Solid-State Characterizations

2.3.1. X-Ray Diffraction (XRD)

The solid-state properties of the SD 30% and PM 30% and individual materials were analyzed using a Miniflex II diffractometer system (Rigaku® Innovative Technologies, Austin, TX, USA) equipped with a copper anode. A thin layer of powder material was dispersed onto a glass carrier. The experimental parameters were a scan rate of 2°/min and 2θ (degree) range of 3–40°.

2.3.2. Scanning Electron Microscopy (SEM)

The morphology of SD 30% and PM 30% was evaluated using a scanning electron microscope (Shimadzu SS-550, Japan) equipped with a field emission gun emitter. Samples were dispersed onto double-coated metalized carbon tape and covered with gold. Secondary electron images were obtained under low vacuum (0.5 torr) at an acceleration voltage of 200 kV.

2.3.3. Differential Scanning Calorimetry (DSC)

Thermograms were obtained using a DSC-60 scanning calorimeter (Shimadzu, Japan) at a heating rate of 10 °C/min from 17–600 °C in 50-mL nitrogen atmosphere. Thermal properties of TMX, SDs, and PM 30% were analyzed.

2.3.4. Fourier-Transform Infrared Spectroscopy (FTIR)

The most promising SD, chosen based on the XRD amorphization results, was used to evaluate the major intermolecular interactions of the TMX–polymer and polymer–polymer mixtures. Analyses were performed using a Spectrum 400 FTIR spectrophotometer (PerkinElmer®, Waltham, MA, USA) with a universal attenuated total reflectance (UATR-FTIR) accessory, composed of a diamond crystal base and zinc selenide-focusing element. Spectra were recorded over the range of 4000 to 400 cm^{-1}, with a resolution of 4 cm^{-1}.

2.4. TMX Equilibrium Solubility

TMX equilibrium solubility in both the presence and absence of the polymer was experimentally determined. Test tubes were filled with 10 mL of hydrochloric acid buffer pH 1.2, phosphate buffer pH 7.4, or phosphate buffer pH 7.4 + Tween 80 (0.4% *w/v*). An excess amount of TMX was added to each tube, which were shaken at 150 rpm in an incubator at 37 ± 0.1 °C for 120 h, then centrifuged at 10,000 rpm for 30 min. The supernatant was removed and diluted whenever necessary to be quantified using a UV spectrophotometer at 274 nm for hydrochloric acid buffer pH 1.2 and phosphate buffer pH 7.4 and 307 nm for phosphate buffer H 7.4 containing Tween 80. In order to determine TMX equilibrium solubility in the presence of polymers, the same procedure was performed with a suspension of TMX +

Eudragit® RL 100, TMX + Eudragit® L 100, and TMX + Eudragit® L 100–Eudragit® RL 100 (1:1, *w/w*). Polymer concentrations were selected based on the TMX drug-loading content in each SD (10%, 20%, and 30%, *w/w*).

2.5. Dissolution Tests

Dissolution profiles of SDs, PM 30%, and crystalline TMX were compared. Supersaturation was maintained through non-sink conditions during the entire test period in order to evaluate the behavior of each SD in relation to the TMX release and possible nucleation and recrystallization events. This method departs from the idea of a limited amount of gastrointestinal fluids during in-vivo release, which contributes to the overall release kinetics from supersaturated drug delivery systems [7]. Dissolution tests were performed in 200 mL of dissolution media at 37 ± 0.5 °C using a VanKel 7010 dissolution system (Agilent Technologies, Santa Clara, CA, USA) equipped with a USP II apparatus on a constant rotational speed of 100 rpm. TMX concentrations were sufficiently quantifiable through UV spectrophotometry in pH 1.2 dissolution medium. In contrast, TMX was not soluble enough in pH 7.4 medium, so Tween 80 (0.4% *w/v*) had to be added to allow spectrophotometric quantification [29]. Aliquots were collected at predefined intervals (10, 20, 30, 40, 60, 120, 180, and 240 min for pH 1.2 medium and 10, 20, 30, 40, 60, 120, 180, 240, 300, and 360 min for pH 7.4 medium) without replacing the medium in order to maintain adequate supersaturation conditions. No more than 10% of the total volume of medium was withdrawn. Samples were filtered using a Millipore® 0.45-μm polyvinyl difluoride (PVDF) syringe filter and analyzed spectrophotometrically at 274 nm (pH 1.2 solution) or 307 nm (pH 7.4 solutions). Measurements were performed in triplicate, and dissolution results are presented as mean ± standard deviation. A dimensionless sink index (SI) was used to adjust the degree of deviation from sink conditions in all dissolution tests [30] according to the following equation:

$$SI = \frac{C_s \times V}{D} \quad (1)$$

where "C_s" is the equilibrium solubility of crystalline TMX with respect to each dissolution medium, "V" is the volume of dissolution medium, and "D" is the total amount of drug in the test sample. The isolated TMX, SDs, and PM 30% masses inserted into each dissolution test were calculated according to the crystalline TMX equilibrium solubility in each medium (see Section 3.3), departing from a SI value of 0.33 [31]. For instance, this resulted in approximately 3 times the mass required to reach TMX equilibrium solubility in each medium.

3. Results and Discussion

3.1. Solid-State Characterizations

To investigate the drug-loading threshold in the SDs with the polymer blends, the amount of drug in each system was raised up to 30% (*w/w*), and XRD analysis was conducted. Figure 1 shows the XRD patterns of crystalline TMX, PM 30%, and SDs. As expected from a crystalline-organized structure, TMX showed distinct intense peaks corresponding to the polymorph II of the drug [32]. These peaks also appeared in the diffractogram of PM 30%, although with lower intensity, indicating that the components of the amorphous polymer blend were present but not capable of preventing drug crystallites to co-exist, which is due to the thick polymer coating around the coated particles, which could weaken the signals, as these polymers have amorphous characteristics [33,34].

Diffractograms of SDs 10%, 20%, and 30% indicated that the dispersion of TMX into the polymer matrices allowed their mixing at a molecular level, as evidenced by the observed amorphous profiles, which is desirable for enhancing the solubility and stability of the drug in the matrix due to possible chemical interactions and reduced molecular mobility [7,35]. This is further confirmed through SEM analysis.

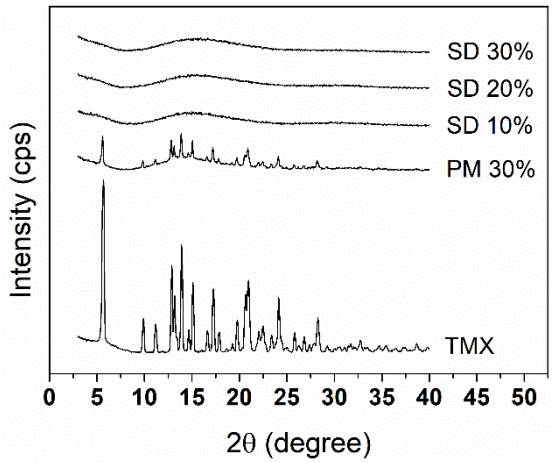

Figure 1. X-ray diffraction (XRD) diffractogram patterns of solid dispersions (SDs) 10%, 20%, and 30%; physical mixture (PM) 30%; and crystalline tamoxifen (TMX).

SEM images (Figure 2) provided information on the solid state, particle shape, size, and surface characteristics and confirmed the effectiveness of the solvent evaporation process to obtain the SD systems. Samples were examined under different magnifications, because each system contained particles of various sizes as a result of their multicomponent composition. Although higher magnification darkened the field of view for the physically mixed particles, it allowed us to investigate the structural details of each sample.

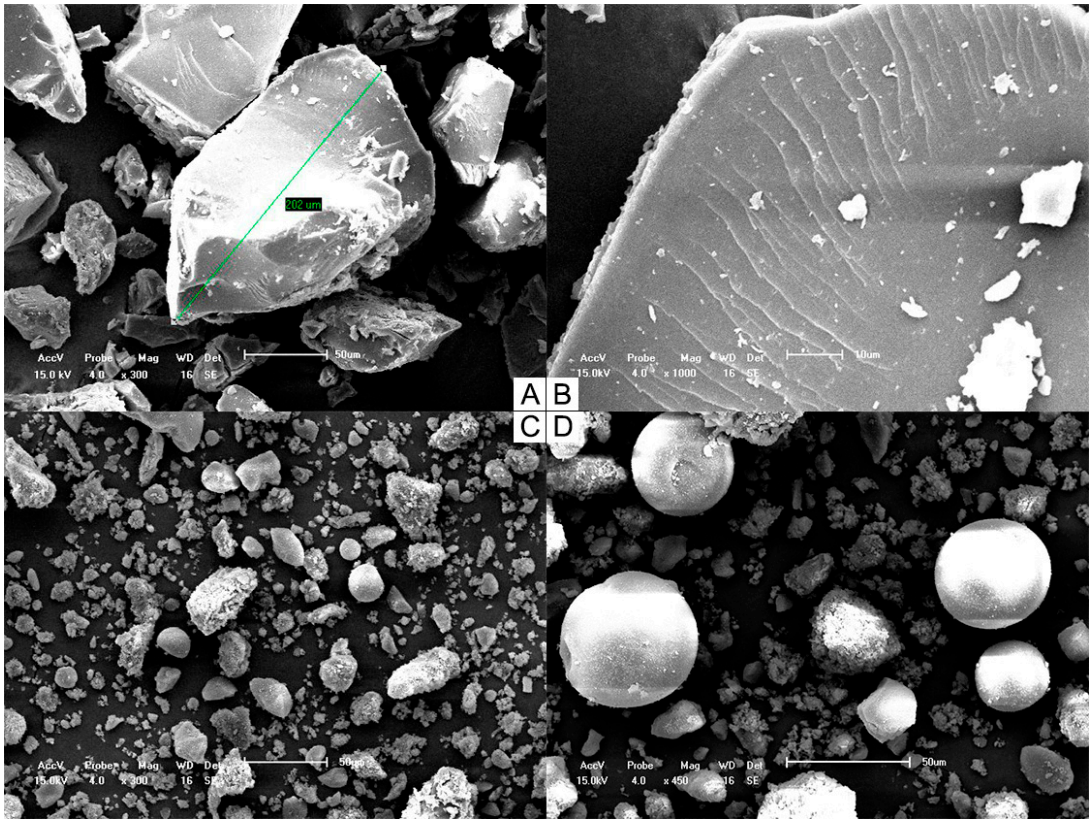

Figure 2. Scanning electron micrographs of both SD 30% (**A**) 300× and (**B**) 1000× and PM 30% (**C**) 300× and (**D**) 450×.

SD 30% was composed of small but relatively uniform particles, which is probably due to the grinding and sieving steps used in the preparation process. A few cracks were observed on the surfaces

of particles, but the superficial layer was otherwise smooth, in accordance with the formation of a single-phase homogeneous system with TMX dispersed within the matrix. PM 30% was formed by separated components of distinct shapes.

DSC curves of SDs, PM 30%, and isolated TMX (Figure 3A), along with Binary SD and isolated polymers (Figure 3B) were analyzed to understand differences in glass transition (Tg) behavior due to material mixing and interactions. The DSC analysis of TMX revealed the occurrence of an endothermic event between 142.68 °C and 155 °C, corresponding to the melting point of the drug [36]. For PM 30%, the event was observed at 140.97 °C. However, in SD 10%, SD 20%, and SD 30%, TMX did not exhibit the endothermic melting range, which indicates that the drug should be dispersed within the polymer matrix, forming only one phase—also supported by XRD analyses.

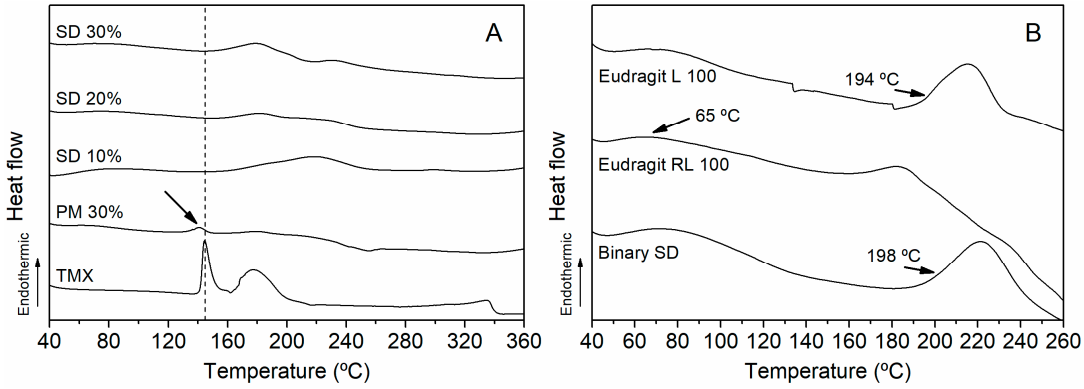

Figure 3. Differential scanning calorimetry (DSC) curves of (**A**) SDs, PM 30%, and isolated TMX, along with (**B**) Eudragit® L 100 and Eudragit® RL 100.

Eudragit® RL 100 showed a Tg temperature around of 65 °C while the Tg of Eudragit® L 100 was 195 ºC, as previously reported [37]. Binary SD had a higher Tg (198 °C) than Eudragit® RL 100 and around Eudragit L® 100, because the latter has a longer chain length, which influences the glass transition of the shorter chain (Eudragit RL® 100); this is due to interactions and miscibility between polymers [34,35]. In the case of SDs with variable drug loadings, there was no significant change in Tg behavior.

3.2. Fourier-Transform Infrared

FTIR analyses were conducted to investigate possible interactions between the different components. When comparing the TMX FTIR spectrum with those of SD 30% and PM 30% (Figure 4A), it can be noticed that there was no evidence of chemical interactions of the drug with the polymers based on the absence of band shifts. This result probably arose from the absence of proton donor and acceptor groups in the TMX chemical structure [36].

FTIR spectra of isolated polymers and their combinations through solvent cast (Binary SD) are presented in Figure 4B. Eudragit® L 100 showed an absorption band in the region of 3521 cm^{-1} to 3230 cm^{-1} related to its OH group. Compared to Eudragit® L 100, Binary SD had a marked reduction in band intensity in this region, suggesting a possible interaction between OH groups and the C=O of Eudragit® RL 100 (1731 cm^{-1}). The OH–carbonyl interaction can be facilitated by the lack of OH groups in Eudragit® RL 100; it impairs the self-interaction of Eudragit® RL 100 and increases its availability to interact with Eudragit® L 100.

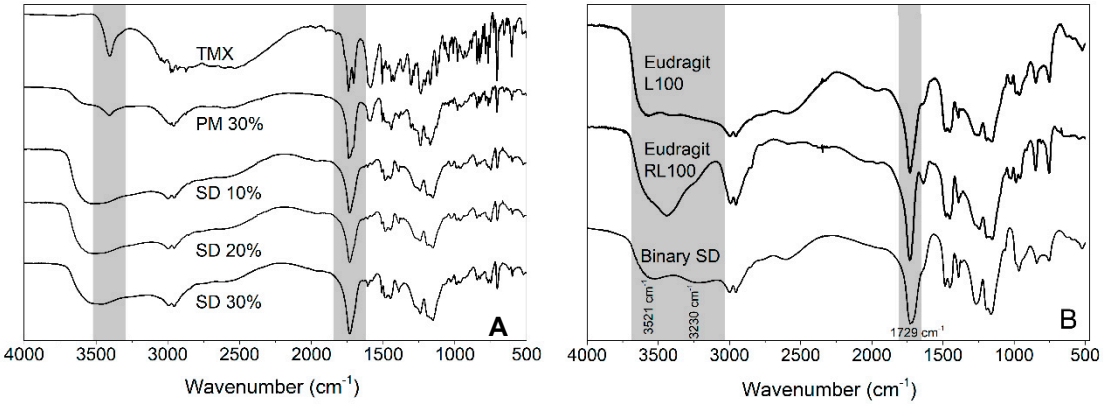

Figure 4. (**A**) Fourier-transform infrared (FTIR) spectra of isolated TMX, PM 30%, SD 10%, SD 20%, and SD 30%. (**B**) FTIR spectra of Eudragit® L 100, Eudragit® RL 100, and Binary SD.

3.3. TMX Equilibrium Solubility

The equilibrium solubility of crystalline TMX was determined in both the presence and absence of polymers in each employed dissolution media. TMX demonstrated a higher solubility in HCl medium pH 1.2 (25.01 ± 2.17 μg·mL^{-1}) when compared to phosphate buffer pH 7.4 (17.11 ± 2.58 μg·mL^{-1}). As expected, the addition of Tween 80 surfactant (0.4%, *w/v*) to the basic medium promoted an increase in TMX solubility (280.17 ± 2.57 μg·mL^{-1}) (Figure 5). This effect can be caused by the alternating polar regions of TMX, which consist of continuous citrate matrices and molecular apolar fragments of the drug's hydrocarbons. When TMX is in a solution with Tween 80, it is incorporated into the apolar nucleus of micelles, which increases the partitioning of the drug into the medium and, consequently, its solubility.

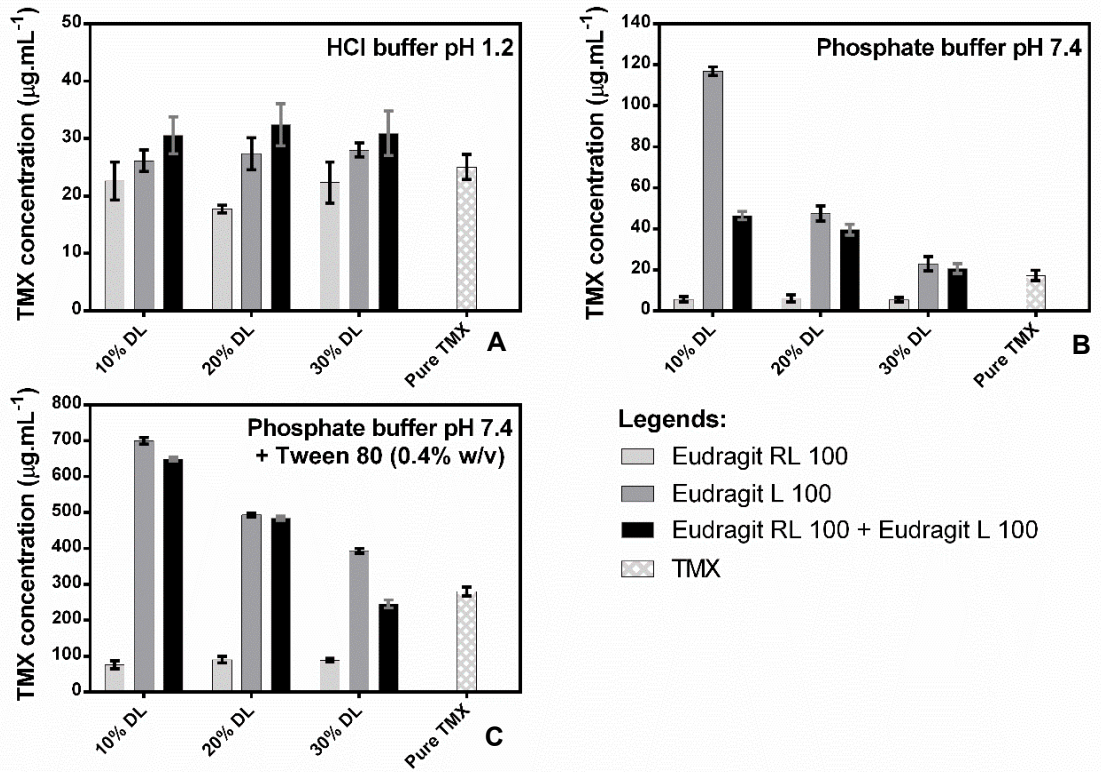

Figure 5. Equilibrium solubility of crystalline TMX in the absence or presence of presuspended polymers in HCl buffer pH 1.2 (**A**), phosphate buffer pH 7.4 (**B**), and phosphate buffer pH 7.4 + Tween 80 0.4% (*w/v*) (**C**). Polymer concentrations were adjusted based on 10%, 20%, or 30% drug-loading (DL) systems during dissolution.

Addition of the polymers to the pH 1.2 medium (Figure 5A) did not seem to improve TMX solubility, regardless of the concentration. However, the addition of Eudragit® L 100 increased TMX solubility in a concentration-dependent manner in the pH 7.4 medium (Figure 5B) and in the pH 7.4 medium containing Tween 80 (0.4% *w/v*) (Figure 5C). Eudragit® RL 100, on the other hand, decreased the concentration of solubilized TMX in the pH 7.4 medium from 17.16 ± 2.58 $\mu g \cdot mL^{-1}$ to 5.43 ± 1.18 $\mu g \cdot mL^{-1}$ as a consequence of the low solubility of Eudragit® RL 100 and the swelling of the polymer when in the solution, which can decrease drug solubilization in the medium, which may be attributed to the absence of a drug–polymer interaction, reducing the driving force for drug dissolution. This result agrees with the decrease in the concentration of TMX in the solution promoted by the addition of the two polymers. A similar result was found with Dehghani et al., 2017 when verifying the decrease of the cinnarizine drug with Eudragit RL 100, reducing this dissolution driving force of the drug and occurring its precipitation in the medium.

3.4. Dissolution Study under Non-Sink Conditions

Dissolution tests under non-sink conditions were performed in order to investigate the kinetic solubility profiles of TMX released from different SDs prepared with the polymer mixtures (Figure 6). As demonstrated before, TMX has different equilibrium solubilities in each tested dissolution medium (either pH 1.2 or pH 7.4 + Tween 80), which were taken into account when standardizing the degree of supersaturation in the dissolution method. The use of a dimensionless SI (i.e., the degree of departure from sink conditions) allowed us to analyze the distinct behavior in each media.

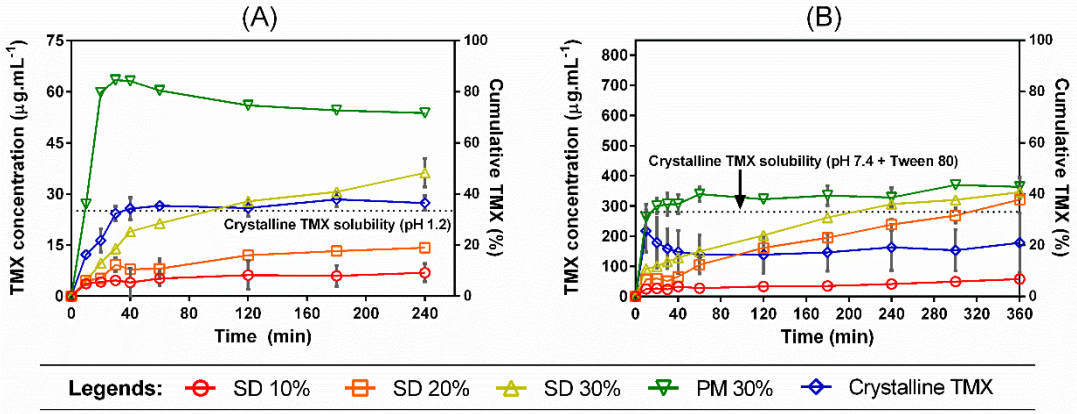

Figure 6. Dissolution profiles under non-sink conditions of crystalline TMX, SDs, and PM 30% in (**A**) HCl pH 1.2 buffer and (**B**) phosphate buffer pH 7.4 + Tween 80 (0.4% *w/v*). The dotted line represents the TMX equilibrium solubility in each dissolution medium. Error bars represent the standard deviation.

In both dissolution media, SD 30% achieved the highest cumulative release when compared to the other SDs, 10% and 20%. However, the physical mixture PM 30% was able to outperform all SDs in the TMX release in both situations, with a more pronounced efficiency in pH 1.2 media. Not only slower, the TMX kinetic solubility from the SDs had also a lower maximum concentration (C_{max}) than the PM 30%, which exhibited a small decline in drug concentration when in pH 1.2. In this case, a better extent of TMX supersaturation was achieved by the physical mixture, which was obtained through direct mixing of the components' powders instead of going through the process of film casting. This may possibly be due to the polymer–polymer interactions promoted through the SD preparation steps, which can affect drug mobility and hinder drug release from the final polymer matrix. Nevertheless, a better dissolution efficiency (DE%) (Table 1) was achieved by the PM 30%, followed by the SDs in decreasing drug-loading order. DE (%) can be defined by Equation (2):

$$DE\% = \frac{AUC}{\text{Total rectangle area}} \times 100 \quad (2)$$

where AUC is the area under the curve achieved by each system, and the total rectangle area refers to each dissolution graph, obtained by multiplying the maximum of X and Y values.

Table 1. Maximum concentration (C_{max}), area under the curve (AUC), and DE (%) obtained by the dissolution of each system in pH 1.2 and 7.4.

System	pH 1.2			pH 7.4		
	C_{max} (μg.mL^{-1})	AUC	DE (%) *	C_{max} (μg.mL^{-1})	AUC	DE (%) *
SD 10%	6.9	1328	7.38	57.9	13,600	4.72
SD 20%	14.2	2572	14.29	321	68,209	23.68
SD 30%	36.2	6014	33.41	345.5	86,764	30.13
PM 30%	63.4	13,106	72.81	369.3	118,962	41.31
TMX	28.4	6051	33.62	216.9	54,718	19

* DE (%): dissolution efficiency calculated based on the total rectangle's area from each dissolution graph in Figure 6 (pH 1.2: 18,000 and pH 7.4: 288,000), using Equation (2).

Regarding the drug loadings, higher C_{max} and AUC were observed with increasing drug loadings. The effects of drug loading on kinetic solubility profiles of poorly soluble drugs released from amorphous SDs were thoroughly investigated before [38–40], where a lower drug loading (near 10% or less) usually leads to a faster release and a higher maximum concentration, with a consequent faster and sharper recrystallization after trespassing the drug C_s. This is especially the case when single-soluble polymers are used to prepare amorphous SDs, since a polymer dissolution-mediated mechanism is observed with low drug loadings (i.e., the overall kinetic solubility profile is a result of polymer dissolution). With a single water-soluble polymer as the SD carrier, a lower drug loading can be associated with lesser SD hydrophobicity, since poorly soluble drugs are hydrophobic, which facilitates the polymer dissolution into the media and generates a faster degree of supersaturation. This was not the case observed in our study, since not only a water-insoluble polymer (Eudragit RL 100) was used to prepare the SDs, but it was also mixed with a second component, which can further change the final behavior. Insoluble polymers are known for their diffusion-controlled release by which the polymer swelling takes place as the main factor associated with the drug release. Furthermore, since we fixed the polymer proportion in our study, a drug loading-mediated release seems to dominate the kinetic solubility profiles, where the drug loading dictated both the dissolution rate and C_{max} in ascending order.

Crystalline TMX was not able to reach its equilibrium solubility in pH 7.4 in the course of the dissolution time, even considering the presence of the Tween 80 surfactant, which normally facilitates drug dissolution by reducing the surface tension between the hydrophobic drug and water. This suggests that, although the TMX equilibrium solubility is higher in this pH when compared to acidic media, as demonstrated in Section 3.3 (also considering the presence of Tween 80), it takes longer to reach the equilibrium value when in the presence of the polymer carriers.

4. Conclusions

The viability of mixing TMX with two hydrophobic amorphous polymers was investigated. Experimental and theoretical studies have shown the interaction of the two meth(acrylate) polymers through the -OH groups by hydrogen bonding. This interaction affected the functional properties of the polymers at contact with the dissolution medium. We evidenced a reduction in TMX crystalline solubility in the presence of Eudragit RL 100. In-vitro dissolution tests showed that the dissolution performance was dependent on the drug loading at each SD system. Thus, the present study can help to better understand the importance of polymer–polymer interactions, the ability to alter drug solubility, and is important for investigating processes that may involve multi-component polymer–polymer and polymer–polymer drugs.

Author Contributions: Conceptualization, methodology, validation, formal analysis, and investigation: D.T.C.d.S., D.N., L.J.d.A.D., and A.C.Q.d.M.V.; writing—original draft preparation, D.T.C.d.S., D.N., L.J.d.A.D., A.C.Q.d.M.V., P.S., M.F.L.R.S., J.L.S.-S., and E.B.S.; and supervision, writing—review and editing, project administration, resources, and funding acquisition, P.S., M.F.L.R.S., J.L.S.-S., and E.B.S. All authors have made a substantial contribution. All authors have read and agreed to the published version of the manuscript.

Funding: This work was funded by the Coordenação de Aperfeiçoamento de Pessoal de Nível Superior (CAPES/Brazil), by the Portuguese Science and Technology Foundation (FCT/MCT), and European Funds (PRODER/COMPETE) under the projects M-ERA-NET/0004/2015 and UIDB/04469/2020 (strategic fund) and co-financed by FEDER under the Partnership Agreement PT2020.

Acknowledgments: The authors thank the CETENE Center for the support on characterization techniques.

Conflicts of Interest: The authors declare no conflict of interest.

References

1. Huh, W.J.; Khurana, S.S.; Geahlen, J.H.; Kohli, K.; Waller, R.A.; Mills, J.C. Tamoxifen Induces Rapid, Reversible Atrophy, and Metaplasia in Mouse Stomach. *Gastroenterology* **2012**, *142*, 21–24.e7. [CrossRef] [PubMed]
2. Mendonsa, N.; Almutairy, B.; Kallakunta, V.R.; Sarabu, S.; Thipsay, P.; Bandari, S.; Repka, M.A. Manufacturing strategies to develop amorphous solid dispersions: An overview. *J. Drug Deliv. Sci. Technol.* **2020**, *55*, 101459. [CrossRef]
3. Cho, H.-W.; Baek, S.-H.; Lee, B.-J.; Jin, H.-E. Orodispersible Polymer Films with the Poorly Water-Soluble Drug, Olanzapine: Hot-Melt Pneumatic Extrusion for Single-Process 3D Printing. *Pharmaceutics* **2020**, *12*, 692. [CrossRef]
4. Gordhan, D.; Swainson, S.M.; Pearce, A.K.; Styliari, I.D.; Lovato, T.; Burley, J.C.; Garnett, M.C.; Taresco, V. Poly (Glycerol Adipate): From a Functionalized Nanocarrier to a Polymeric-Prodrug Matrix to Create Amorphous Solid Dispersions. *J. Pharm. Sci.* **2020**, *109*, 1347–1355. [CrossRef] [PubMed]
5. Xie, T.; Taylor, L.S. Dissolution Performance of High Drug Loading Celecoxib Amorphous Solid Dispersions Formulated with Polymer Combinations. *Pharm. Res.* **2016**, *33*, 739–750. [CrossRef]
6. Obeidat, W.M.; Obeidat, S.M.; Al-Zoubi, N. Investigations on the Physical Structure and the Mechanism of Drug Release from an Enteric Matrix Microspheres with a Near-Zero-Order Release Kinetics Using SEM and Quantitative FTIR. *AAPS PharmSciTech* **2009**, *10*, 615–623. [CrossRef] [PubMed]
7. Sun, D.D.; Lee, P.I. Haste Makes Waste: The Interplay Between Dissolution and Precipitation of Supersaturating Formulations. *AAPS J.* **2015**, *17*, 1317–1326. [CrossRef] [PubMed]
8. Pawar, J.; Tayade, A.; Gangurde, A.; Moravkar, K.; Amin, P.D. Solubility and dissolution enhancement of efavirenz hot melt extruded amorphous solid dispersions using combination of polymeric blends: A QbD approach. *Eur. J. Pharm. Sci.* **2016**, *88*, 37–49. [CrossRef]
9. Nurunnabi, M.; Parvez, K.; Nafiujjaman, M.; Revuri, V.; Khan, H.A.; Feng, X.; Lee, Y.-K. Bioapplication of graphene oxide derivatives: Drug/gene delivery, imaging, polymeric modification, toxicology, therapeutics and challenges. *RSC Adv.* **2015**, *5*, 42141–42161. [CrossRef]
10. Khdair, A.; Hamad, I.; Alkhatib, H.; Bustanji, Y.; Mohammad, M.; Tayem, R.; Aiedeh, K. Modified-chitosan nanoparticles: Novel drug delivery systems improve oral bioavailability of doxorubicin. *Eur. J. Pharm. Sci.* **2016**, *93*, 38–44. [CrossRef]
11. Pang, X.; Jiang, Y.; Xiao, Q.; Leung, A.W.; Hua, H.; Xu, C.S. pH-responsive polymer–drug conjugates: Design and progress. *J. Control. Release* **2016**, *222*, 116–129. [CrossRef] [PubMed]
12. Louage, B.; Nuhn, L.; Risseeuw, M.D.; Vanparijs, N.; De Coen, R.; Karalic, I.; Van Calenbergh, S.; De Geest, B.G. Well-Defined Polymer-Paclitaxel Prodrugs by a Grafting-from-Drug Approach. *Angew. Chem. Int. Ed.* **2016**, *55*, 11791–11796. [CrossRef] [PubMed]
13. Kumar, B.; Deeba, F.; Priyadarshi, R.; Bano, S.; Kumar, A.; Negi, Y.S. Development of novel cross-linked carboxymethyl cellulose/poly(potassium 1-hydroxy acrylate): Synthesis, characterization and properties. *Polym. Bull.* **2019**, *77*, 4555–4570. [CrossRef]
14. Séon-Lutz, M.; Couffin, A.-C.; Vignoud, S.; Schlatter, G.; Hébraud, A. Electrospinning in water and in situ crosslinking of hyaluronic acid / cyclodextrin nanofibers: Towards wound dressing with controlled drug release. *Carbohydr. Polym.* **2019**, *207*, 276–287. [CrossRef]
15. Martinez, A.W.; Caves, J.M.; Ravi, S.; Li, W.; Chaikof, E.L. Effects of crosslinking on the mechanical properties, drug release and cytocompatibility of protein polymers. *Acta Biomater.* **2014**, *10*, 26–33. [CrossRef]

16. Falde, E.J.; Freedman, J.D.; Herrera, V.L.; Yohe, S.T.; Colson, Y.L.; Grinstaff, M.W. Layered superhydrophobic meshes for controlled drug release. *J. Control. Release* **2015**, *214*, 23–29. [CrossRef]
17. Alhijjaj, M.; Belton, P.; Qi, S. An investigation into the use of polymer blends to improve the printability of and regulate drug release from pharmaceutical solid dispersions prepared via fused deposition modeling (FDM) 3D printing. *Eur. J. Pharm. Biopharm.* **2016**, *108*, 111–125. [CrossRef]
18. Mustafin, R.I. Interpolymer combinations of chemically complementary grades of Eudragit copolymers: A new direction in the design of peroral solid dosage forms of drug delivery systems with controlled release (review). *Pharm. Chem. J.* **2011**, *45*, 285–295. [CrossRef]
19. Siepmann, J.; Siepmann, J.; Walther, M.; Macrae, R.; Bodmeier, R. Polymer blends for controlled release coatings. *J. Control. Release* **2008**, *125*, 1–15. [CrossRef]
20. Wulff, R.; Leopold, C. Coatings from blends of Eudragit® RL and L55: A novel approach in pH-controlled drug release. *Int. J. Pharm.* **2014**, *476*, 78–87. [CrossRef]
21. Boyd, B.J.; Bergström, C.A.; Vinarov, Z.; Kuentz, M.; Brouwers, J.; Augustijns, P.; Brandl, M.; Bernkop-Schnürch, A.; Shrestha, N.; Préat, V.; et al. Successful oral delivery of poorly water-soluble drugs both depends on the intraluminal behavior of drugs and of appropriate advanced drug delivery systems. *Eur. J. Pharm. Sci.* **2019**, *137*, 104967. [CrossRef] [PubMed]
22. Ramírez-Rigo, M.V.; Olivera, M.E.; Rubio, M.; Manzo, R.H. Enhanced intestinal permeability and oral bioavailability of enalapril maleate upon complexation with the cationic polymethacrylate Eudragit E100. *Eur. J. Pharm. Sci.* **2014**, *55*, 1–11. [CrossRef] [PubMed]
23. Nollenberger, K.; Albers, J. Poly(meth)acrylate-based coatings. *Int. J. Pharm.* **2013**, *457*, 461–469. [CrossRef]
24. Souto, E.B.; Da Da Ana, R.; Souto, S.B.; Zielinska, A.; Marques, C.; Andrade, L.N.; Horbańczuk, O.K.; Atanasov, A.G.; Lucarini, M.; Durazzo, A.; et al. In Vitro Characterization, Modelling, and Antioxidant Properties of Polyphenon-60 from Green Tea in Eudragit S100-2 Chitosan Microspheres. *Nutrients* **2020**, *12*, 967. [CrossRef] [PubMed]
25. Tambosi, G.; Coelho, P.F.; Luciano, S.; Lenschow, I.C.S.; Zétola, M.; Stulzer, H.K.; Pezzini, B.R. Challenges to improve the biopharmaceutical properties of poorly water-soluble drugs and the application of the solid dispersion technology. *Matéria* **2018**, *23*. [CrossRef]
26. Ullah, F.; Javed, F.; Othman, M.; Rehman, S.U.; Ahmad, Z.; Akil, H.M. Star-shaped self-assembled micelles of block copolymer [chitosan-co-poly(ethylene glycol) methyl ether methacrylate] hydrogel for hydrophobic drug delivery. *Polym. Bull.* **2017**, *75*, 2243–2264. [CrossRef]
27. Balogh, A.; Farkas, B.; Domokos, A.; Farkas, A.; Démuth, B.; Borbás, E.; Nagy, B.; Marosi, G.; Nagy, Z.K. Controlled-release solid dispersions of Eudragit® FS 100 and poorly soluble spironolactone prepared by electrospinning and melt extrusion. *Eur. Polym. J.* **2017**, *95*, 406–417. [CrossRef]
28. Tran, T.T.; Tran, P.H.-L. Controlled Release Film Forming Systems in Drug Delivery: The Potential for Efficient Drug Delivery. *Pharmaceutics* **2019**, *11*, 290. [CrossRef]
29. Dehghani, F.; Farhadian, N.; Golmohammadzadeh, S.; Biriaee, A.; Ebrahimi, M.; Karimi, M. Preparation, characterization and in-vivo evaluation of microemulsions containing tamoxifen citrate anti-cancer drug. *Eur. J. Pharm. Sci.* **2017**, *96*, 479–489. [CrossRef]
30. Sun, D.D.; Ju, T.-C.R.; Lee, P.I. Enhanced kinetic solubility profiles of indomethacin amorphous solid dispersions in poly(2-hydroxyethyl methacrylate) hydrogels. *Eur. J. Pharm. Biopharm.* **2012**, *81*, 149–158. [CrossRef]
31. Figueirêdo, C.B.M.; Nadvorny, D.; Vieira, A.C.Q.D.M.; Soares-Sobrinho, J.L.; Neto, P.J.R.; Lee, P.I.; Soares, M.F.D.L.R. Enhancement of dissolution rate through eutectic mixture and solid solution of posaconazole and benznidazole. *Int. J. Pharm.* **2017**, *525*, 32–42. [CrossRef] [PubMed]
32. Gamberini, M.C.; Baraldi, C.; Tinti, A.; Palazzoli, F.; Ferioli, V. Vibrational study of tamoxifen citrate polymorphism. *J. Mol. Struct.* **2007**, *840*, 29–37. [CrossRef]
33. Chen, D.; Singh, D.; Sirkar, K.K.; Pfeffer, R. Continuous preparation of polymer coated drug crystals by solid hollow fiber membrane-based cooling crystallization. *Int. J. Pharm.* **2016**, *499*, 395–402. [CrossRef] [PubMed]
34. Dereymaker, A.; Cinghia, G.; Mooter, G.V.D. Eudragit® RL as a stabilizer for supersaturation and a substrate for nanocrystal formation. *Eur. J. Pharm. Biopharm.* **2017**, *114*, 250–262. [CrossRef] [PubMed]
35. Baghel, S.; Cathcart, H.; O'Reilly, N.J. Polymeric Amorphous Solid Dispersions: A Review of Amorphization, Crystallization, Stabilization, Solid-State Characterization, and Aqueous Solubilization of Biopharmaceutical Classification System Class II Drugs. *J. Pharm. Sci.* **2016**, *105*, 2527–2544. [CrossRef] [PubMed]

36. Altmeyer, C.; Karam, T.K.; Khalil, N.M.; Mainardes, R.M. Tamoxifen-loaded poly(L-lactide) nanoparticles: Development, characterization and in vitro evaluation of cytotoxicity. *Mater. Sci. Eng. C* **2016**, *60*, 135–142. [CrossRef]
37. Parikh, T.; Gupta, S.S.; Meena, A.; Serajuddin, A.T.M. Investigation of thermal and viscoelastic properties of polymers relevant to hot melt extrusion—III: Polymethacrylates and polymethacrylic acid based polymers. *J. Excip. Food Chem.* **2014**, *5*, 56–64.
38. Indulkar, A.S.; Lou, X.; Zhang, G.G.Z.; Taylor, L.S. Insights into the Dissolution Mechanism of Ritonavir–Copovidone Amorphous Solid Dispersions: Importance of Congruent Release for Enhanced Performance. *Mol. Pharm.* **2019**, *16*, 1327–1339. [CrossRef]
39. Lin, X.; Su, L.; Li, N.; Hu, Y.; Tang, G.; Liu, L.; Li, H.; Yang, Z. Understanding the mechanism of dissolution enhancement for poorly water-soluble drugs by solid dispersions containing Eudragit® E PO. *J. Drug Deliv. Sci. Technol.* **2018**, *48*, 328–337. [CrossRef]
40. Han, Y.R.; Lee, P.I. Effect of Extent of Supersaturation on the Evolution of Kinetic Solubility Profiles. *Mol. Pharm.* **2016**, *14*, 206–220. [CrossRef]